SSCL-Preprint-494

SSCL-Preprint-494
August 1993
Distribution Category: 400

A. Yücel
J. Maddocks

Thermal Conductivity of Commercially Available 21-6-9 Stainless Steel

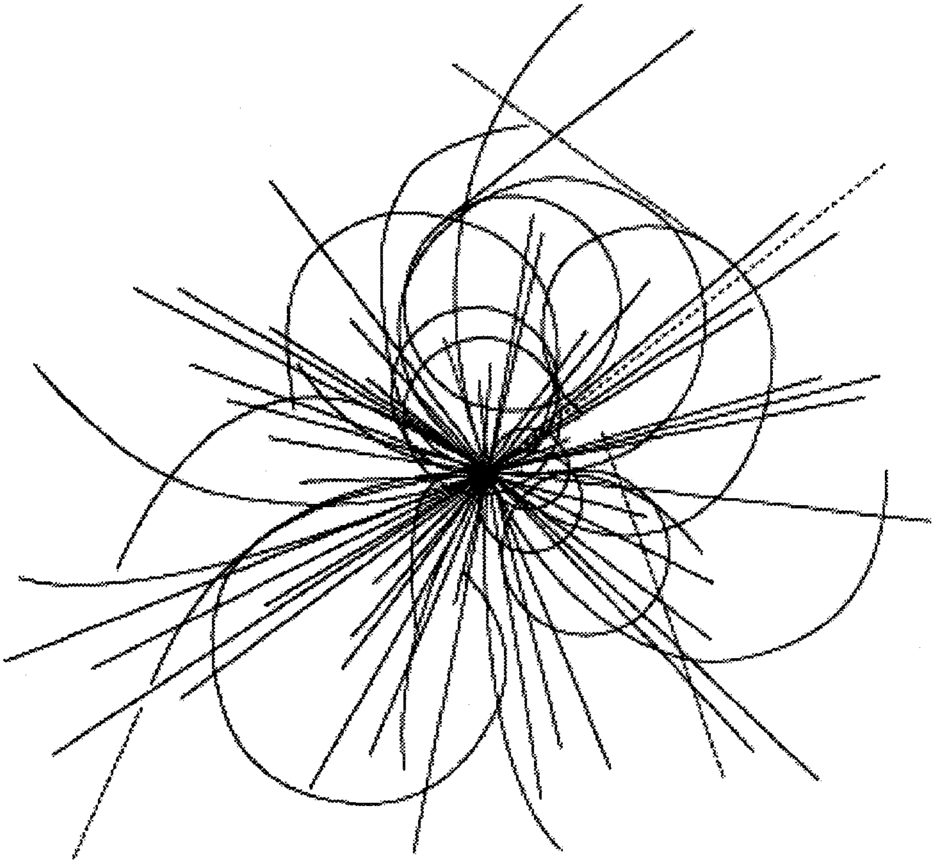

Superconducting Super Collider Laboratory

APPROVED FOR RELEASE OR
PUBLICATION - O.R. PATENT GROUP
BY.............DATE 4/3/95..

SSCL-Preprint-494

Thermal Conductivity of Commercially Available 21-6-19 Stainless Steel*

A. Yücel and J. Maddocks

Superconducting Super Collider Laboratory†
2550 Beckleymeade Ave.
Dallas, TX 75237

August 1993

---

*Submitted to the "Plenum Publishing Corporation" August, 1993.

†Operated by the Universities Research Association, Inc., for the U.S. Department of Energy under Contract No. DE-AC35-89ER40486.

ww

THERMAL CONDUCTIVITY OF COMMERCIALLY AVAILABLE 21-6-9 STAINLESS STEEL

A. Yücel and J. R. Maddocks

Superconducting Super Collider Laboratory*
2550 Beckleymeade Avenue
Dallas, Texas 75237

ABSTRACT

Thermal conductivity values of 21-6-9 stainless steel over the temperature range of 5 K to 120 K are reported. Thermal conductivity integrals are measured using a steady-state heat flux method. The resulting data are fit with a polynomial and differentiated to obtain the conductivity. The derived conductivity is compared to published data for high-manganese stainless steels and to data for other stainless steels. A discussion of the methodology and its accuracy is included.

INTRODUCTION

The literature contains limited and somewhat conflicting data[1–4] on the thermal conductivity of nitrogen-strengthened, high-manganese stainless steels. One such alloy, 21-6-9 steel, is being considered for cryogenic application in the cold mass of Superconducting Super Collider magnets. This work presents the results of thermal conductivity integral measurements on commercial samples of 21-6-9 (Nitronic 40) steel.

MEASUREMENT APPARATUS AND PROCEDURE

Two samples of Nitronic 40 were tested. The first was cut from a section of tubing specified only as Nitronic 40. The second sample was machined from a piece of mill annealed bar stock. The composition of Sample 2 is listed in Table 1, together with the acceptable composition ranges for 21-6-9 stainless steels.

The dimensions of each sample are nominally the same and have been chosen to keep the time constant reasonably short for reaching steady state, while maximizing the value of the temperature difference across the samples. The dimensions chosen (1.1 mm thick, 6.4 mm wide, and 60.2 mm long) resulted in a time constant near room temperature of 1 h.

---

*Operated by the Universities Research Association, Inc., for the U.S. Department of Energy under Contract No. DE-AC35-89ER40486.

Table 1. Composition of 21-6-9 stainless steels, and Sample 2.

	C	Mn	P	S	Si	Cr	Ni	N
XM-10	0.080 max.	8.00–10.00	0.060 max.	0.030 max.	1.00 max.	19.00–21.5	5.50–7.50	0.15–0.40
XM-11	0.040 max.	8.00–10.00	0.060 max.	0.030 max.	1.00 max.	19.00–21.5	5.50–7.50	0.15–0.40
Sample 2	0.044	8.92	0.017	0.001	0.44	19.26	7.24	0.27

Each specimen was soldered between two copper mounting blocks and fastened to the bottom plate of a vacuum can, as indicated in Figure 1. Two different methods of fastening were used. In the first two experimental runs (Sample 1), the lower copper mounting block was covered with copper-impregnated grease and pressed firmly onto the stainless steel bottom plate of the vacuum can. When immersed in the helium bath it was frozen in place. However, two problems arose with this method. First, the bottom end temperature of the sample rose above 10 K at relatively modest heat fluxes. Second, upon thermally recycling from 4 K to room temperature and back to 4 K, good thermal contact with the bottom of the vacuum can was lost. To remedy these problems in subsequent runs (Sample 2), a copper bottom plate was used on the vacuum can and the sample assembly was bolted to it. Again, copper impregnated grease was used to improve thermal contact. This arrangement proved to be quite satisfactory.

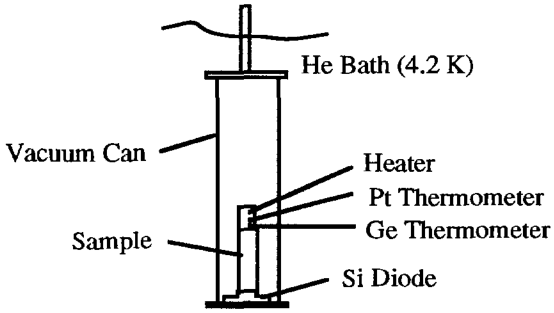

Figure 1. Schematic representation of apparatus showing sample location and instrumentation.

Experimental instrumentation consisted of three thermometers and a heater. The heater was a metal film resistor inserted in the upper copper mounting block of the sample assembly and held in place with GE varnish. Two thermometers, one germanium and one platinum, were also located in the upper copper mounting block. They were thermally anchored in grease so they could be removed without damage. A silicon diode was located in the lower mounting block and was used to monitor the bottom end temperature. All instrumentation leads were Phosphor-bronze wire, thermally anchored to the bath. Heat conduction through the leads was negligible over the entire range of temperatures investigated.

After installing the instrumentation and mounting the samples, a room temperature insulating vacuum of approximately 1×10^{-6} Torr was established, using a diffusion pump. The entire vacuum can assembly was then placed in a dewar where it was precooled to approximately 120 K before transfering liquid helium. During transfer of helium, the insulating vacuum remained open to a leak detector. Once the apparatus was fully immersed in liquid and no leaks have been observed, the detector was valved off. In this way, we ensured that the pressure in the vacuum can is less than 1×10^{-6} Torr and that gas conduction from the heated sample to the bath was negligible.

The apparatus was then allowed to come to thermal equilibrium and the readings of all thermometers are compared. The saturated bath temperature was determined by monitoring the atmospheric pressure inside and outside the dewar. These measurements typically agreed within ± 3 Torr. In all cases the silicon diode in the base of the sample agreed with the bath temperature to within ± 0.05 K, which is the extent of its accuracy. The germanium thermometer, however, was systematically higher than the bath temperature by approximately 0.15 K. This resulted partly from heat leaking down the instrumentation leads past the 4.2 K anchor and partly from 300 K radiation coming down the vacuum pumpout line. The magnitude of this parasitic heating was estimated to be 5 μW and was negligible even at the lowest heater powers reported.

The heater was powered with a dc voltage supply. A precision resistor in series with the heater provided a means of measuring the current, which together with the applied voltage provided a measure of the heat input. When the steady state was achieved, the heat input as well as the temperatures were recorded. In this way, thermal conductivity integrals were measured for warm end temperatures ranging from 5 K to 140 K.

When the heater was turned on, temperatures rose slowly to steady-state values. The time required to achieve steady state was dependent on the average temperature of the sample and was on the order of hours for warm end temperatures above 100 K. As a matter of practice, then, the heater was turned up to full capacity and the warm end temperature was monitored until it was close to a desired value. The power was then gradually reduced until a steady temperature was achieved. The accuracy of this method has been verified on a number of occasions by allowing the perceived steady state to remain for at least 2 h. Since the time constant associated with reaching steady state increases with increasing temperature, the inaccuracies introduced by this method will be worst at the highest heater powers. Thus, the verification tests were always conducted at high heat inputs. In all cases, temperatures changed by less than 50 mK.

In addition to uncertainties arising from an unsteady state, parallel heat leaks may occur through instrumentation leads, through the insulating vacuum, and by radiation to the wall of the vacuum can. As previously indicated, care was taken to minimize heat losses through instrumentation leads and gas conduction. Finally, we note that the small surface area of the sample assembly, together with the relatively low temperature range investigated, combined to make radiation losses negligible as well.

RESULTS

Thermal conductivity integrals obtained for Samples 1 and 2 are listed in Tables 2 and 3, respectively. The tables also include the corresponding temperatures at the upper (T_U) and lower (T_L) ends. As discussed above, T_L rose above the bath temperature for Sample 1, but remained very close to the bath temperature for Sample 2.

Table 2. Thermal conductivity integrals for Sample 1.

Data point i	$T_{L,i}$ (K)	$T_{U,i}$ (K)	$Q_{meas,i}$ (W/m)	Data point i	$T_{L,i}$ (K)	$T_{U,i}$ (K)	$Q_{meas,i}$ (W/m)
1	4.218	6.09	0.849	16	9.848	78.39	326.594
2	4.238	7.15	1.513	17	9.988	79.87	337.505
3	4.258	8.24	2.339	18	4.735	15.14	10.684
4	4.258	8.25	2.347	19	5.485	23.73	30.127
5	4.288	9.13	3.112	20	5.905	27.97	41.738
6	4.308	10.11	4.096	21	6.365	32.23	56.185
7	4.708	20.02	20.477	22	6.775	35.51	68.513
8	6.108	39.78	88.839	23	7.325	40.03	88.203
9	9.588	78.84	330.559	24	8.605	49.96	136.669
10	4.328	10.13	4.076	25	9.905	59.98	194.940
11	4.338	10.51	4.481	26	11.195	69.83	259.698
12	4.748	20.00	20.415	27	13.775	90.00	413.576
13	4.768	20.39	21.313	28	15.005	99.74	497.068
14	6.238	39.73	88.177	29	19.765	130.00	795.625
15	6.288	40.31	90.615	30	20.915	139.88	918.565

Table 3. Thermal conductivity integrals for Sample 2.

Data point i	$T_{L,i}$ (K)	$T_{U,i}$ (K)	$Q_{meas,i}$ (W/m)	Data point i	$T_{L,i}$ (K)	$T_{U,i}$ (K)	$Q_{meas,i}$ (W/m)
1	4.28	91.64	464.398	34	4.21	43.39	110.639
2	4.26	83.74	390.604	35	4.22	47.92	134.778
3	4.24	74.30	297.285	36	4.23	52.02	162.733
4	4.21	63.47	233.951	37	4.23	54.21	174.229
5	4.19	53.01	163.502	38	4.25	60.00	212.906
6	4.17	43.94	110.816	39	4.20	47.81	135.107
7	4.16	32.62	57.813	40	4.23	60.09	213.307
8	4.19	53.40	168.115	41	4.23	63.78	239.469
9	4.16	36.36	75.730	42	4.25	72.66	308.579
10	4.14	24.06	30.291	43	4.24	68.22	270.763
11	4.26	85.04	405.418	44	4.26	76.24	335.488
12	4.29	96.93	530.256	45	4.27	80.24	370.582
13	4.34	115.18	731.882	46	4.28	84.52	409.076
14	4.18	5.53	0.576	47	4.30	90.25	452.844
15	4.18	6.14	0.905	44	4.31	94.70	501.468
16	4.18	7.01	1.449	49	4.32	99.74	552.286
17	4.18	7.52	1.805	50	4.35	109.62	654.488
18	4.18	8.03	2.188	51	4.39	119.80	768.177
19	4.18	8.57	2.634	52	4.46	139.94	1021.507
20	4.18	9.03	3.038	53	77.14	86.11	73.917
21	4.18	9.46	3.438	54	77.13	91.19	119.872
22	4.18	10.05	4.037	55	77.13	88.44	92.093
23	4.18	12.13	6.462	56	77.14	94.79	152.045
24	4.18	14.09	9.275	57	77.16	100.26	205.045
25	4.18	16.13	12.728	58	77.16	104.23	245.095
26	4.19	18.14	16.692	59	77.15	108.00	283.868
27	4.19	20.00	20.847	60	77.14	112.15	327.801
28	4.19	22.46	27.069	61	77.15	115.69	366.294
29	4.19	24.42	32.221	62	77.15	119.46	406.904
30	4.19	28.23	44.345	63	77.15	123.27	450.940
31	4.20	31.79	57.771	64	77.15	126.65	491.759
32	4.20	35.80	74.867	65	77.15	130.13	533.253
33	4.21	40.11	94.638	66	77.15	134.93	591.356

The combined data for Samples 1 and 2 are fitted with a fourth-order polynomial of the form

$$q(T) \equiv \int_{T_{bath}}^{T} k(\theta)d\theta = \sum_{j=0}^{4} a_j (T - T_0)^j \ , \tag{1}$$

where T is the temperature (K), T_{bath} is the bath temperature fixed at 4.18 K, T_0 is the reference temperature for the curve-fit, and q is the thermal conductivity integral (W/m) from T_{bath} to T. The singular value decomposition method[5] is used to determine the coefficients a_j, which minimized the sum of the squares of the residuals, Σr_i^2. The residual r_i for the i th data point is expressed as $r_i = Q_{meas,i} - Q_{pred,i}$, where $Q_{meas,i}$ is the thermal conductivity integral measured between the lower and upper end temperatures, and $Q_{pred,i}$ is the corresponding value predicted by the curve-fit:

$$Q_{pred,i} \equiv \int_{T_{L,i}}^{T_{U,i}} k(\theta)d\theta = \sum_{j=0}^{4} a_j (T_{U,i} - T_0)^j - \sum_{j=0}^{4} a_j (T_{L,i} - T_0)^j \ . \tag{2}$$

Table 4. Coefficients for thermal conductivity integral curve-fits (Eq. (1)).

	$5\ \mathrm{K} \le T \le 20\ \mathrm{K}$	$20\ \mathrm{K} \le T \le 120\ \mathrm{K}$
a_0	0.0	2.069361E+01
a_1	3.488162E–01	2.319298E+00
a_2	5.580653E–02	6.566394E–02
a_3	4.027611E–04	–1.882401E–04
a_4	–6.165039E–06	2.675137E–07
T_0	4.18 K	20.0 K

A single curve to represent the data over the entire range of interest between 5 K and 120 K could not be obtained. Instead, the data from 5 K to 20 K, and those from 20 K to 120 K, were fitted with separate curves. Continuity in the thermal conductivity integral, as well as in the first (thermal conductivity) and second derivatives of the curves, was maintained at the cut-off temperature of 20 K. Table 4 lists the coefficients obtained for the two temperature ranges.

Figure 2 shows the percentage residuals ($100 \times r_i / Q_{meas,i}$) in the two temperature ranges. The residual plots indicate that the curve-fits are quite satisfactory, within 6% of the data at the high end temperatures. As a further check of the curve-fit in the high temperature range, thermal conductivity integrals were measured by anchoring Sample 2 in an LN_2 bath. These data (points 53 through 66 in Table 3) were compared with predicted values and agreed within 5%.

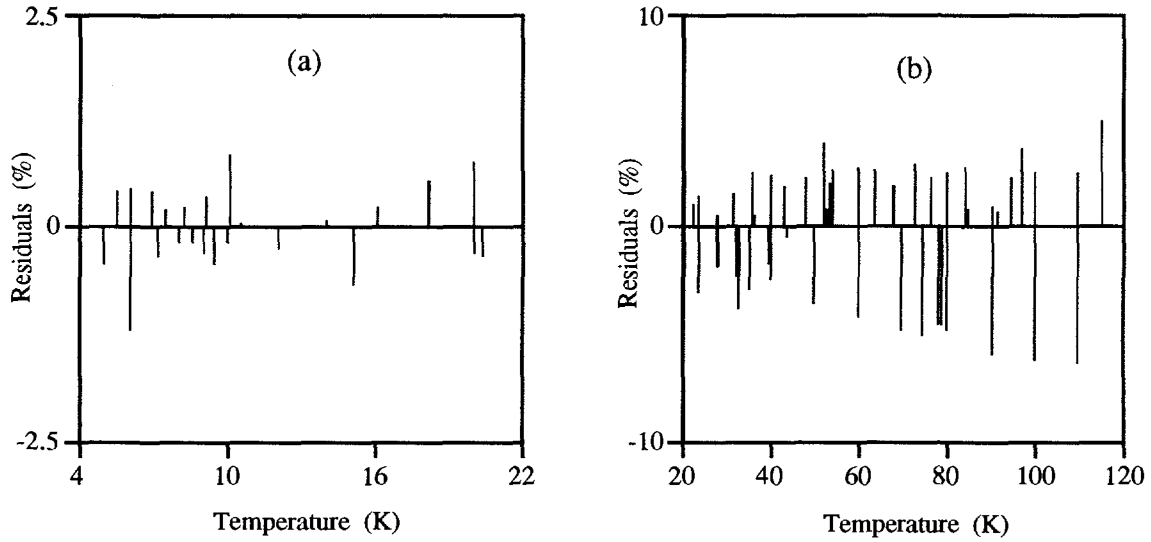

Figure 2. Residual plots: a) $5\ \mathrm{K} \le T \le 20\ \mathrm{K}$, and b) $20\ \mathrm{K} \le T \le 120\ \mathrm{K}$.

Since there are no thermal conductivity integrals reported in the literature for 21-6-9 steel, the present data are compared with integral values recommended for S300 series stainless steels.[6] Figure 3 shows that there is very little difference between the 21-6-9 values obtained in this work and the values for S300 series steels.

The thermal conductivity k at a given temperature T is obtained by differentiating Eq. (1) to yield:

$$k(T) = \sum_{j=1}^{4} j a_j (T - T_0)^{j-1} . \tag{3}$$

This approach is mathematically equivalent to that used by Hust and Lankford.[7] Thermal conductivity values so obtained are shown in Figure 4, together with the thermal

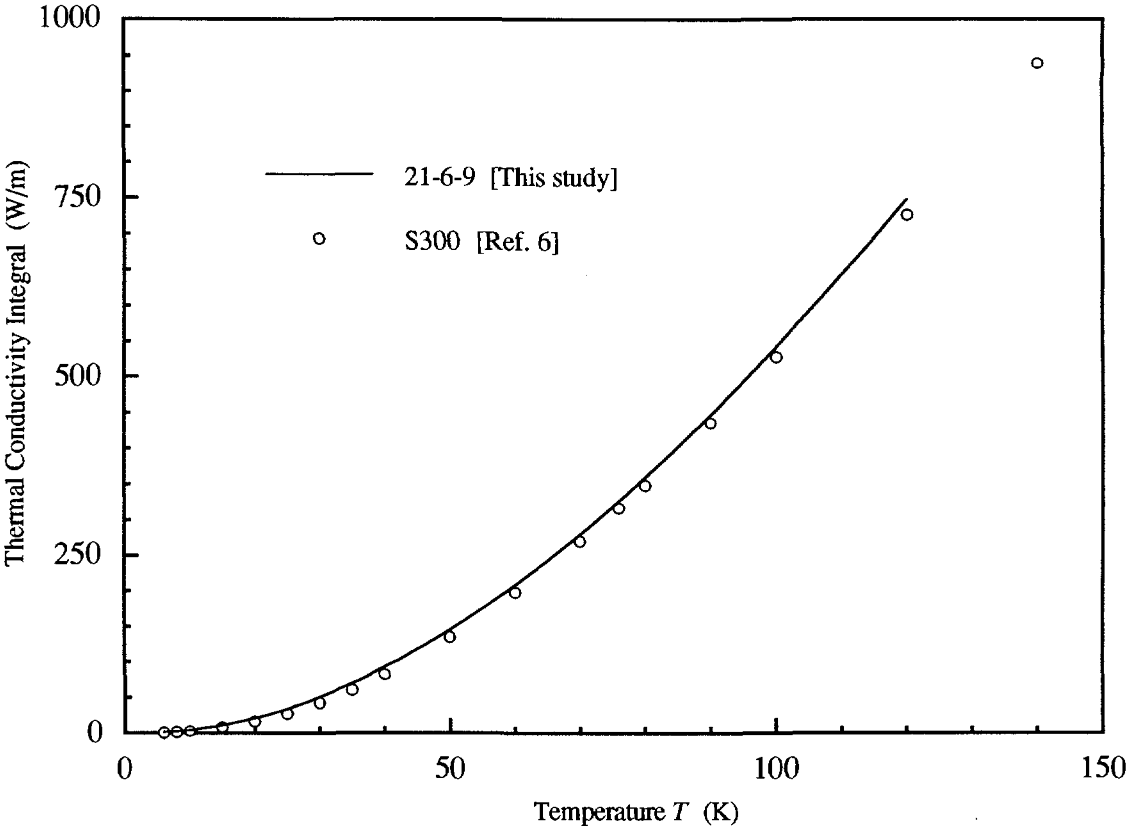

Figure 3. Thermal conductivity integral from 4.18 K to temperature T.

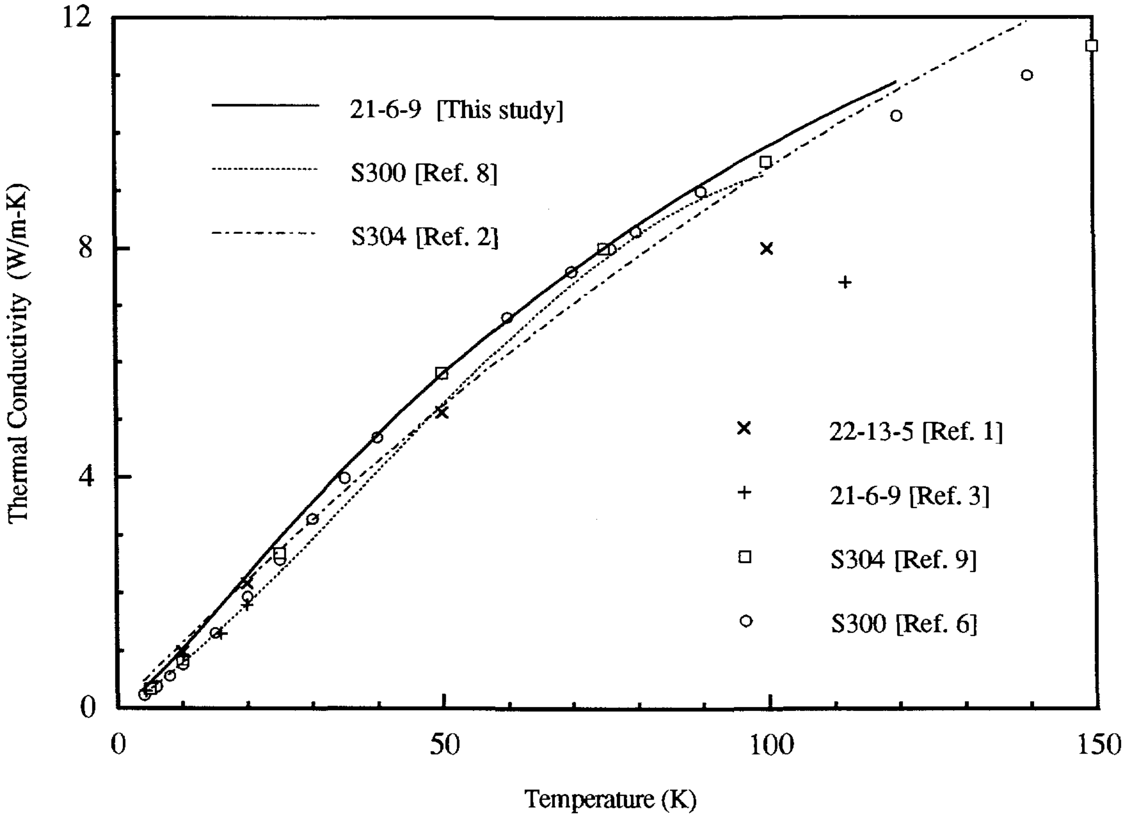

Figure 4. Thermal conductivity of austenitic stainless steels.

conductivity data for various austenitic stainless steels. Values for 21-6-9 steel from the present study correspond closely with those for the S300 steels over the entire temperature range. They are also in good agreement with the few data points available for 21-6-9 and 22-13-5 steels in the low temperature range. However, they differ substantially from the two data points reported for the latter steels near 100 K.

SUMMARY

Thermal conductivity integrals for 21-6-9 stainless steel are reported over the temperature range of 5 K to 140 K. A fourth-order polynomial is fit to the data, and coefficients are determined for the temperature ranges 5–20 K and 20–120 K. These curve-fits are differentiated to obtain values of the thermal conductivity. Both the integrals and the conductivity are compared to series S300 stainless steel values and found to be in good agreement over the entire temperature range investigated. Similar comparisons of data from this report with published values of conductivity for 21-6-9 and 22-13-5 reveal reasonable agreement below 20 K, but considerable differences at temperatures near 100 K.

ACKNOWLEDGEMENTS

The authors are grateful to James Morris and James Briggs for their valuable technical assistance. The authors wish to thank W. J. Schumacher and W. Tobiason of Armco for providing a sample of Nitronic 40.

REFERENCES

1. "Handbook on Materials for Superconducting Machinery," Metals and Ceramics Information Center, Battelle Columbus Laboratories, Columbus, Ohio (1977).
2. N. J. Simon and R. P. Reed, "Structural Materials for Superconducting Magnets," Preliminary Draft, NIST, Boulder, Colorado (1982).
3. Y. Li et al., The microstructure and properties of a cryogenic steel Fe-21Cr-6Ni-9Mn-N, in: "Advances in Cryogenic Engineering (Materials)," Vol. 30, A. F. Clark and R. P. Reed, eds., Plenum Press, New York (1984).
4. O. Umezawa and K. Ishikawa, Electrical and thermal conductivities and magnetization of some austenitic steels, titanium and titanium alloys at cryogenic temperatures, *Cryogenics*, 32:873 (1992).
5. G. E. Forsythe, M. A. Malcolm, and C. B. Moler, "Computer Methods for Mathematical Computations," Prentice-Hall, New York (1977).
6. "A Compendium of the Properties of Materials at Low Temperature (Phase II)," WADD Technical Report 60-56, Part IV (1961).
7. J. G. Hust and A. B. Lankford, Comments on the measurement of thermal conductivity and presentation of a thermal conductivity integral method, *International Journal of Thermophysics*, 3:67 (1982).
8. P. J. Giarratano, V. D. Arp, and R. V. Smith, Forced convection heat transfer to supercritical helium, *Cryogenics*, 11:385 (1971).
9. Y. S. Touloukian, R. W. Powell, C. Y. Ho, and P. G. Klemens, "Thermophysical Properties of Matter," Vol. 1, IFI/Plenum, New York (1970).